An impaired metabolism of nucleotides underpins a novel mechanism of cardiac remodeling leading to Huntington's disease related cardiomyopathy.

Marta Toczek[1], Daniel Zielonka[2], Paulina Zukowska[1], Jerzy T. Marcinkowski[2], Ewa Slominska[1], Mark Isalan[3], Ryszard T. Smolenski [1**], Michal Mielcarek[3*]

[1] Department of Biochemistry, Medical University of Gdansk, 1 Debinki Str, 80-210, Gdansk, Poland.
[2] Department of Social Medicine, Poznan University of Medical Sciences, 6 Rokietnicka Str, 60-806, Poznan, Poland.
[3] Department of Life Sciences, Imperial College London, Exhibition Road, SW7 2AZ, London, UK.

***** Corresponding author: Michal Mielcarek, Department of Life Sciences, Imperial College London, Exhibition road, SW7 2AZ, London, UK, tel. +44 207 59 46482, fax: +44 2075942290,e-mail: mielcarekml@gmail.com; m.mielcarek@imperial.ac.uk

** Co-corresponding author: Ryszard Smolenski, Department of Biochemistry, Medical University of Gdansk, 1 Debinki Str, 80-210, Gdansk, Poland, tel:+48 58 349 14 63, fax: +48 58 349 14 65, e-mail: rt.smolenski@gumed.edu.pl

ABSTRACT

Huntington's disease (HD) is mainly thought of as a neurological disease, but multiple epidemiological studies have demonstrated a number of cardiovascular events leading to heart failure in HD patients. Our recent studies showed an increased risk of heart contractile dysfunction and dilated cardiomyopathy in HD pre-clinical models. This could potentially involve metabolic remodeling, that is a typical feature of the failing heart, with reduced activities of high energy phosphate generating pathways. In this study, we sought to identify metabolic abnormalities leading to HD-related cardiomyopathy in pre-clinical and clinical settings. We found that HD mouse models developed a profound deterioration in cardiac energy equilibrium, despite AMP-activated protein kinase hyperphosphorylation. This was accompanied by a reduced glucose usage and a significant deregulation of genes involved in *de novo* purine biosynthesis, in conversion of adenine nucleotides, and in adenosine metabolism. Consequently, we observed increased levels of nucleotide catabolites such as inosine, hypoxanthine, xanthine and uric acid, in murine and human HD serum. These effects may be caused locally by mutant HTT, via gain or loss of function effects, or distally by a lack of trophic signals from central nerve stimulation. Either may lead to energy equilibrium imbalances in cardiac cells, with activation of nucleotide catabolism plus an inhibition of re-synthesis. Our study suggests that future therapies should target cardiac mitochondrial dysfunction to ameliorate energetic dysfunction. Importantly, we describe the first set of biomarkers related to heart and skeletal muscle dysfunction in both pre-clinical and clinical HD settings.

Keywords: Huntington's disease, cardiomyopathy, arrhythmia, energy imbalance, catabolism of nucleotides, heart failure

SUMMARY

Huntington's disease (HD) is a fatal neurodegenerative disorder caused by a polyglutamine expansion in the huntingtin protein. HD-related cardiomyopathy has been widely described in different mouse models, however there is little known about the source of the pathological remodelling in HD hearts. We found that contractile dysfunction in HD settings might be caused by components of cellular energy imbalance, changes in catabolism of adenine nucleotides, steady-state internal redox derangements and an activation of AMPK, leading to a shift in the cardiac substrate preference. These changes were accompanied by increased concentrations of adenine nucleotide catabolites (inosine, hypoxanthine, xanthine and uric acid) and uridine in both HD mouse models and HD patients' plasma. These metabolites represent the first identified biomarkers related to striated muscle dysfunction in HD. Our study explores a mechanism that might lead to HD-related cardiomyopathy and opens new avenues for therapeutic treatments in HD.

HIGHLIGHTS

- Heart dysfunction in HD is caused by the altered metabolism of nucleotides *in vivo*
- Altered energy imbalances may lead to heart malfunction in HD *in vivo*
- Increased levels of catabolites of nucleotides are potential biomarkers of HD heart dysfunction

1. INTRODUCTION

Huntington's disease (HD) is an inherited neurodegenerative disorder characterized by irrepressible motor dysfunction, cognitive decline and psychiatric disturbances that lead to progressive dementia and death; for a recent review see [1]. The source of HD is a CAG repeat expansion within the huntingtin gene (*HTT*) that translates into a polyglutamine stretch (polyQ) within the Exon-1 of HTT protein [1]. In the human population, the number of wild-type CAG repeats varies from 6 to 35, and the presence of 36 or more repeats defines the pathogenic HD allele [1]. HTT is a 348 kDa multi-domain protein that is normally expressed in various mammalian tissues, with the highest levels in the brain and testes [2]. It is believed that the polyQ expansion within the Exon-1 of HTT produces insoluble toxic aggregates, a hallmark of HD molecular pathology that can be detected in an early pre-symptomatic stage in pre-clinical and clinical settings [3]. These aggregates have been identified in HD brains, as well as in many non-central nervous system tissues [4], but not in hearts [5]. HTT protein is believed to act as a scaffolding protein since many interaction partners have been identified and, based on these findings, it is assumed that HTT is involved in gene transcription, intracellular signaling, trafficking, endocytosis and metabolism [6].

Despite the lack of HTT toxic aggregates in HD hearts, there is strong evidence that heart malfunction can be a potent contributor of HD progression. In fact, several epidemiological studies have indicated that heart failure is the second most common cause of death in HD patients; for a recent review see [7]. Although there is not enough molecular data underpinning such HD-related cardiomyopathy in humans, a recent clinical study published by Stephen and colleagues revealed a significant contractile heart dysfunction [8]. The study was performed on a large cohort of 598 patients with early symptoms of HD, participating in a clinical trial using standard 12-lead electrocardiograms (ECGs). It was found that abnormal ECGs were typical for 25.3% of early symptomatic patients and were manifested by rates of bradycardia, prolonged intra-ventricular conduction, as well as QTC prolongation, likely leading to arrhythmia and aggravated cardiac failure [8]. Importantly, these findings in human HD patients are in line with our previously published study in preclinical settings, where we noticed a contractile heart dysfunction in two symptomatic HD mouse models, namely R6/2 and *Hdh*Q150 [5]. We showed that heart contractile dysfunction was accompanied by a re-expression of foetal genes, apoptotic cardiomyocyte loss, and a moderate degree of interstitial fibrosis [5]. Moreover, we showed that R6/2 HD murine hearts are not able to respond to chronic isoproterenol treatment to the same degree as wild type

hearts, and some of the hypertrophic signals are likely to be attenuated in symptomatic HD animals [9].

It is well established that myocardial contraction depends strongly on the mitochondrial energy supply [10]. This is supported by the fact that 25–35% of the myocardial volume is occupied by mitochondria [11]. Furthermore, proteomic analysis of cardiac mitochondria in patients with dilated cardiomyopathy showed alterations in substrate utilization (glucose, pyruvate and fatty acids) and in energy production [12]. One of the typical features of cardiomyopathy is a reduction in the activity of ATP-producing pathways, which could be intensified by a deficiency of cardiac energy substrates [13]. Therefore, we hypothesized that cardiac nucleotides and energy metabolism might contribute to a novel mechanism leading to HD heart pathology.

In order to identify these new pathological mechanisms, we performed our current studies using the same HD mouse models in which we previously described contractile abnormalities leading to heart failure, namely R6/2 and *Hdh*Q150 [5]. Interestingly, our study underlines the fact that HD-related cardiomyopathy includes components of cellular energy imbalance, changes in catabolism of adenine nucleotides, steady state internal redox derangements and an activation of AMPK, leading to a shift in the cardiac substrate preference. Moreover, cardiac energy metabolism impairment results in increased concentrations of adenine nucleotide catabolites (inosine, hypoxanthine, xanthine and uric acid) and uridine in both HD mouse models and HD patients' plasma. These metabolites represent the first identified biomarkers related to striated muscle dysfunction in HD.

2.MATERIALS AND METHODS

2.1 Mouse maintenance and genotyping

Mouse HD lines were maintained and genotyped as previously described [14], and all experimental procedures performed on mice were conducted under a project license from the Home Office, UK, and approved by ethical committee at Imperial College London, and by the Medical University of Gdansk Ethics Committee for Animal Experiments. Experimental groups included the R6/2 mouse model at 12 weeks of age (n=5), their C57BL/6J congenic lines littermates (n=5) and the *Hdh*Q150 HD mouse model at 22 months of age (n=5), compared to their C57BL/6J littermates (n=5).

2.2 HD patients and control subjects

Plasma samples from HD patients and control patients (n=5 per group) were obtained from the Polish centre of the European Huntington's Disease Network in Poznan, and approved by the local bioethical board. Written informed consent was obtained from all subjects according to the International Conference on Harmonisation – Good Clinical Practice (ICH-GCP) guidelines (http://www.ich.org/LOB/media/MEDIA482.pdf). HD patients and healthy control subjects that were matched for age, sex, and body mass index (BMI) were enrolled in the presented study. Details about HD patients and control subjects are provided in Supplementary Table 2.

2.3 Measurement of nucleotides and corresponding levels of catabolites in murine heart and serum

Prior to extraction, heart samples were placed for 24 hours in a freeze dryer (Modulyo, Thermo Electron Corporation, USA), at -55°C. Freeze-dried fragments of hearts were extracted with 0.4 M perchloric acid in 1:10 ratio, followed by neutralization with 2 M KOH. Murine blood samples were collected from IVC (lat. *Inferior vena cava*) and centrifuged at 2000 × g for 5 minutes. The obtained volumes of serum varied between 20-50 μL. Next, serum components were extracted with 1.3 M perchloric acid (1:1 ratio). Levels of nucleotides were measured by a reverse phase-high pressure liquid chromatography (RP-HPLC) method using the LC system (Agilent Technologies 1100 series, USA), as described previously [15]. Results are presented as nmol/mg of dry tissue for heart samples and as μM for mouse serum.

2.4 Measurement of nucleotides and corresponding levels of catabolites in human plasma

For blood sample collection, a cannula was inserted into an antecubital vein in HD patients, or control subjects, and 2-3 mL blood samples were collected. Tubes were centrifuged at 2000 × g at 20ºC for 5 min, and plasma was stored at -80ºC. Subsequently, plasma sample components were extracted with 1.3 M perchloric acid (1:1 ratio). Levels of nucleotides were measured by a reverse phase-high pressure liquid chromatography (RP-HPLC) method using the LC system (Agilent Technologies 1100 series, USA), as described above (2.3). Results are presented as μM.

2.5 Cardiac substrate preference study

1,6-^{13}C-glucose (Cambridge Isotope Laboratories, Cambridge UK) was dissolved in PBS as 20% (w/v) solution and injected subcutaneously at a final dose of 3 ml/kg. Two hours after injection, mice were deeply anesthetized with Isoflurane, hearts were freeze-clamped and extracted with 0.4 M perchloric acid. Simultaneously, blood samples were collected from a tail vein before and after 2 hours of ^{13}C-glucose administration. Blood extraction was performed using ice-cooled acetone in a 1:3 ratio. Next, samples were centrifuged at 4°C, 11000 × g for 10 minutes, followed by drying in a vacuum concentrator (JW Electronic, Poland) and sediments were dissolved in high purity water (Nano pure - ultra pure water system, Barnstead, Thermo, USA).

The heart extracts were analyzed by liquid chromatography mass spectrometry using a TSQ-Vantage triple quadrupole mass detector (Thermo, USA), linked to a Surveyor chromatography system (Thermo, USA) [16]. The chromatography column (Phenomenex Synergi Hydro RP 5 mm × 2 mm) was maintained at 25°C. Mobile phases consisted of the phases A: 5 mM of nona–fluoropentanoic acid (NFPA) and B: 0.1% (v/v) formic acid in acetonitrile. Initially, to equilibrate the chromatography system, the column was eluted with a phase composed of 90% buffer A and 10% B. After two minutes, phase composition was 70% A, 30% B. These chromatography conditions were held for 4.5 minutes and then the gradient elution comprised only 100% buffer B. Mobile phase flow rate was 200 μl/min and the injection volume was 2 μl. Mass detection was carried out in positive heated electrospray ionization with fragmentation mode (Tandem MS), monitoring ^{13}C isotopic enrichment of fragments containing C3 of alanine or C4 of glutamate.

The ^{13}C glucose enrichment in blood was measured using liquid chromatography mass spectrometry - LCQ - Deca XP mass detector (Thermo Finnigan, USA). Chromatography

column (Agilent, USA) (Zorbax NH_2, 50 mm × 2.1 mm); temperature was 25°C. Mobile phases consisted of the following buffers: A: 5 mM ammonium acetate and 5 mM ammonium hydroxide; B: 100% acetonitrile. First, to equilibrate the chromatography system, the column was eluted with a phase composed of 10% buffer A and 90% B. After 4 minutes, phase composition was 40% A, 60% B. These conditions were held for 5 minutes and then the gradient elution return to initial conditions. Mobile phase flow rate was 300 µl/min and the injection volume was 2µl. Fragments containing ^{12}C and ^{13}C glucose were detected in negative electrospray ionization with Selected Ion Monitoring Mode.

2.6 Analysis of AMPK phosphorylation level

AMPK phosphorylation was detected using a commercial AMPK alpha pThr172 ELISA kit (Abcam, UK) according to the manufacturer's instructions. Hearts were thoroughly rinsed in PBS to remove blood, followed by a mechanical homogenization. Briefly, hearts were homogenized with an extraction buffer in a 1:5 ratio (tissue:extraction buffer), incubated for 20 minutes on ice, and then centrifuged at 11000 × g at 4°C for 10 minutes. Subsequently, the supernatants were diluted in an incubation buffer in a 1:4 ratio (supernatant:incubation buffer) and used for ELISA reactions. Absorbance was measured at 550 nm with a microplate reader (Synergy HT, BioTek, UK).

2.7 RNA extraction and Taqman real-time PCR expression analysis

Total RNA from heart was extracted with the mini-RNA kit according to the manufacturer's instructions (Qiagen, UK). The reverse transcription reaction was performed using MMLV superscript reverse transcriptase (Invitrogen, USA) and random hexamers (Sigma, USA), as described elsewhere [17]. All Taqman qPCR reactions (Cycler DNA Engine, Peltier Thermal Cycler, Bio-Rad, USA) were performed as described previously. Estimation of mRNA copy number was determined in triplicate for each RNA sample by comparison with the geometric mean of three endogenous housekeeping genes (Primer Design, UK), as described [17].

2.8 Statistical analysis

Values were presented as mean ± SEM. Statistical analysis was performed using paired Student *t* tests (InStat software, GraphPad, USA). A *p*-value of 0.05 was considered to be a significant difference.

3. RESULTS

3.1 A shift in energy equilibrium and nucleotide metabolism in HD mouse model hearts

To address metabolic events contributing to HD-related cardiomyopathy, we used two well-established HD mouse models. Hence, we analyzed heart metabolic profiles in the R6/2 mouse model that is transgenic for a mutated N-terminal Exon 1 HTT fragment [18] and in *Hdh*Q150 mice that have an expanded CAG repeat inserted into the mouse huntingtin gene [19]. For R6/2 mice, we studied the heart metabolic profile in symptomatic animals at 12 weeks of age, while *Hdh*Q150 homozygotes were assessed at the end-stage of disease (22 months). To evaluate the energy shift in hearts within HD mouse models, we measured levels of major adenine nucleotides such as adenosine triphosphate (ATP), adenosine diphosphate (ADP), adenosine monophosphate (AMP), phosphocreatine (PCr) and creatine [19]. ATP is required for normal cardiac function and we found a significant reduction in the ATP level in both HD mouse models (Fig. 1A), in comparison to their wild type littermates, while the level of ADP remained unchanged (Fig. 1B). Cardiac AMP levels were increased only in R6/2 but not *Hdh*Q150 mice (Fig. 1C). Consequently, we plotted our results as ATP/ADP ratio and found a significant reduction in both HD mouse models (Fig. 1D).

The creatine kinase/phosphocreatine system has been reported to play a major role in the control of ATP levels in response to an energy demand [20]. Therefore, we determined the phosphocreatine and creatine levels in the hearts of HD mouse models and found phosphocreatine levels to be significantly decreased while creatine levels (Fig. 1E), and the PCr/Cr ratio (Fig. 1F), remained unaffected. Interestingly, we observed only a trend towards reduction of the total pool of adenine nucleotides (Fig. 2A) but not guanine nucleotides (Fig. 2B) in both HD mouse models. The guanine-to-adenine ratio was significantly increased in the heart in *Hdh*Q150 but not in R6/2 mice (Fig. 2C).

To investigate the steady-state internal redox status in HD hearts, we assessed the levels of oxidized and reduced forms of nicotinamide adenine dinucleotides (NAD+/NADH). We established that NADH levels were significantly lower in the hearts of both HD mouse models (Fig. 2D) while the NAD+ levels showed only a trend towards lowering (Fig. 2E). Subsequently, we found that the NADH/NAD+ ratios were significantly lower in the hearts of R6/2 and *Hdh*Q150 mice (Fig. 2F).

Next, we hypothesized that reduced levels of nucleotides in HD hearts might be accompanied by an increased concentration of their catabolites in serum. Indeed, we found elevated concentrations with up to 100-fold higher levels of inosine, hypoxanthine, xanthine and uric acid in HD mouse models, in comparison to their wild type littermates (Fig. 3A). In

addition, we found elevated levels of uridine; this has elsewhere been described as a biomarker of altered bioenergetics (Fig, 3B) [21]. The uridine phenomenon was observed despite there being no significant changes in the concentrations of adenine nucleotides, such as NAD+ and NADH in HD mouse serum (Supplementary Table 1). Overall, our current study clearly identified alterations in the levels of nucleotides and their catabolites, in diseased HD hearts.

3.2 Increased concentrations of hypoxanthine and uridine in the plasma of HD patients

Following on from these findings, we assessed the concentrations of major adenine nucleotides like ATP and ADP, as well nicotinamide adenine dinucleotides, like NAD+, in the plasma of symptomatic HD patients and control subjects (Supplementary Table 3). We observed diminished concentrations of ATP and no significant differences in the levels of other adenine nucleotides and NAD+, between patient and control plasma. Uric acid levels in the plasma from HD patients showed no differences compared with healthy controls (Fig. 4A). In contrast, hypoxanthine and uridine levels revealed major differences between HD patients and healthy subjects (Fig. 4B, 4E). We observed prominently increased levels of hypoxanthine and uridine in HD plasma, in comparison to that from healthy controls.

Interestingly, hypoxanthine levels strongly correlated with HD disease burden ([Maximum CAG_n - 35.5] × age at examination) (Fig. 4D) and with CAG repeat length (Fig. 4C). We also detected a correlation between uridine levels and CAG repeat length (Fig. 4F), but no correlation with disease burden (Fig. 4G). Moreover, hypoxanthine levels strongly correlated with HD disease duration and negatively correlated with motor score and intensity of chorea (Supplementary Figure 1). Additionally, uridine levels positively correlated with HD disease duration and negatively correlated with motor score and intensity of chorea (Supplementary Figure 2). Increased levels of hypoxanthine and uridine in HD patients' plasma suggested their intensive release from peripheral tissues and reaffirmed the imbalance in energy metabolism that we observed in mouse models.

3.3 Altered cardiac substrate preference and AMPK phosphorylation in HD mouse models

A metabolic failure might often result in a global imbalance between catabolic and anabolic signals, as well as a shift in substrate preference. To better understand the nature of metabolic abnormalities in HD hearts, we assessed glycolysis efficiency based on ^{13}C alanine enrichment after administration of $1^{-13}C$ glucose, as previously described [14]. We found no changes in the ratio of [^{13}C alanine enrichment in the heart] to [^{13}C glucose enrichment in the

blood] in either HD mouse models (Fig. 5A). This confirmed that there were no differences in the cardiac glucose-to-pyruvate flux.

Next, we employed an assay for ^{13}C glutamate enrichment after administration of $^{1\text{-}13}C$ glucose in murine hearts, measuring any alterations in the Krebs cycle as previously described [14]. The analysis revealed that the ratio of [^{13}C glutamate enrichment in the heart] to [^{13}C glucose enrichment in the blood] decreased significantly in both HD mouse models (Fig. 5B), which suggested an elevated α-ketoglutarate labelling. Furthermore, the altered Krebs cycle flux could be explained by a decreased ratio of [^{13}C glutamate] to [^{13}C alanine] enrichment in the hearts of HD mouse models (Fig. 5C).

One of the key players involved in myocardial metabolism is AMP-activated protein kinase (AMPK) that is a major regulatory kinase controlling numerous pathways of energy metabolism [22]. We therefore used protein extracts from *in situ* snap-frozen hearts to establish the phosphorylation level of AMPK in HD mouse models. We found that phosphorylation levels of AMPK in protein lysates from HD hearts were significantly higher than in wild type hearts (Fig. 5D). Together, these results confirmed altered cardiac substrate metabolism in both of the investigated HD mouse models.

3.4 Transcriptional remodeling of genes involved in the synthesis and catabolism of nucleotides

To further unravel the source of metabolic failure in the hearts of HD mouse models, we determined the expression levels of selected genes that are typically altered in different types of mitochondriopathies. In addition, we have previously reported that murine HD hearts are significantly enriched for genes encoding mitochondrial components, as judged by RNA-seq analyses [5], and these were also assayed.

Of 5 tested transcripts that have been shown to be involved in *de novo* purine biosynthesis [23], only 3 transcripts, namely *Adsl (*Adenylosuccinate lyase*), Adlssl1 (*Adenylosuccinate lyase 1) and *Gart* (Phosphoribosylglycinamide formyltransferase), were significantly down-regulated in HD hearts (Fig. 6A). Meanwhile, *Ppart (*Phosphoribosyl pyrophosphate amidotransferase*)* and *Prpsap2 (*Phosphoribosyl pyrophosphate synthetase-associated protein 2*)* remained unchanged. Notably, there was no change in the expression of *Aprt* mRNA *(*Adenine phosphoribosyltransferase*)* in the hearts of HD mouse models; this gene is involved in the purine nucleotide salvage pathway (Fig. 6A) [24].

Next, we examined the transcript levels of genes involved in the conversion of adenine to guanine nucleotides, such as *Gmps (*Guanosine monophosphate synthetase*), Impdh2* (inosine monophosphate dehydrogenase 2*)* and *Gmpr (*Guanosine monophosphate reductase) [25, 26].

We found that only *Gmps* transcripts were significantly decreased in both HD mouse model hearts, while *Gmpr* transcripts were increased only in R6/2 mice and *Impdh2* transcripts remained unchanged (Fig. 6B). In addition, we studied the expression level of transcripts of *Ak1* (Adenylate kinase 1) that is involved in the inter-conversion of adenine nucleotides and plays an important role in cellular energy homeostasis [27]. We found that *Ak1* mRNA was reduced by approximately 50% in HD hearts (Fig. 6B).

We also validated the expression profiles of selected genes involved the catabolism of myocardial nucleotides, such as *Ada (*Adenosine deaminase) and *Dpp4* (Dipeptydyl peptidase-4); both genes are known to be involved in the adenosine degradation pathway [28, 29]. Both transcripts showed a significant up-regulation ($p<0.01$ for the *Ada* transcript and $p<0.001$ for *Dpp4*) in R6/2 and *Hdh*Q150 murine hearts (Fig. 7A). On the other hand, we did not detect any changes in the transcription levels of other genes involved in adenosine synthesis and metabolism, such as *Adk* (Adenosine kinase) and *Nt5e* (Ecto-5'-nucleotidase), in either HD mouse model (Fig. 7A). There was a significant ($p<0.05$) down-regulation of transcripts involved in adenine nucleotide synthesis and conversion, such as *Entpd2* (Ectonucleoside triphosphate diphosphohydrolase 2) and *Nme3* (Nucleoside diphosphate kinase 3) [30, 31], but only in the *Hdh*Q150 mouse model ($p<0.05$) (Fig. 7B). *Nme1* (Nucleoside diphosphate kinase 1), *Nme2* (Nucleoside diphosphate kinase 2) and *Ampd3* (Adenosine monophosphate deaminase 3) transcripts remained unchanged in both HD mouse models (Fig. 7B).

We were also interested in validating the transcriptional profiles of genes engaged in guanine, inosine and hypoxanthine degradation pathways, such as *Gda* (Guanine deaminase), *Pnp* (Purine nucleoside phosphorylase) and *Xdh* (Xanthine dehydrogenase) [32, 33]. We found that all transcripts that are involved in these pathways were unaltered in the hearts of HD mouse models (Fig. 7C).

Finally, to further examine the source of the energy shift in the HD hearts, we studied the transcriptional profile of key players involved in energy metabolism. Hk2 (Hexokinase 2) catalyses the phosphorylation of glucose, the rate-limiting first step of glycolysis and is known as a molecule involved in energy metabolism and cellular protection [34]. *Hk2* transcripts were significantly down-regulated in HD hearts (Fig. 7D). There were no changes in the expression of *Ppargc1a* (Peroxisome proliferator-activated receptor gamma coactivator 1-alpha) and *Ppara* (Peroxisome proliferator-activated receptor alpha) mRNAs, while *Prkaa1* (AMP- activated protein kinase) transcripts were significantly up-regulated in the hearts of HD mouse models (Fig.7D). Taken together, these data indicate a transcriptional remodelling

of genes involved in *de novo* purine biosynthesis, in the purine nucleotide salvage pathway and in catabolism of nucleotides.

4. DISCUSSION

Although HD has been described primarily as a neurological disorder, there is solid evidence emphasizing the contribution of peripheral pathology to disease progression, including skeletal muscle atrophy [35] and heart failure [7]. In fact, recent clinical data confirmed the presence of contractile heart dysfunction in HD pre-symptomatic patients [8], that might lead to HD-related cardiomyopathy or even a cardiac sudden death. On the other hand, there are examples from studies based on HD animal models that have affirmed cardiac pathological events such as brady- and tachyarrhythmias, variations in heart rates and cardiac remodelling [5] and these are in line with the clinical data [8]. However, there is still an urgent need for more insights into the molecular pathologies that might lead to heart malfunction in HD patients.

In pre-clinical settings, the R6/2 mouse model - that displays impairment in cardiac functions - had significant alterations in mitochondrial structure, including the loss of mitochondrial elongated shapes and diffused mitochondrial densities [36, 37]. These morphological changes may lead directly to cardiac energy metabolism imbalances. Indeed, a recent study suggested that cardiac Fas-dependent and mitochondria-dependent apoptotic pathways were activated in R6/2 hearts [38]. Mitochondrial structure disarrangement may thus result in an energy status imbalance in cardiomyocytes.

This type of energy imbalance is not only restricted to the heart but also underpins a decline in an energy metabolism and decreased oxidation in skeletal muscles [14], and is a feature similar to muscle wasting syndrome in cancer cachexia [39]. HD subjects also showed a deficit in mitochondrial oxidative metabolism in skeletal muscles, as judged by a significant decrease in phosphocreatine recovery after exercise [40]. Additionally, *in vitro* muscle cell cultures exhibited abnormalities in mitochondrial membrane potential and cytochrome 3 release [41].

Following on from these findings, we found a reduced cardiac ATP level, combined with a lower ATP/ADP ratio in two HD mouse models of varying severity (R6/2, *Hdh*Q150). Interestingly, a reduced ATP level has already been positively associated with the severity of human heart failure [42] and a decreased ATP pool was also observed in heart tissue obtained from patients with a dilated and restricted cardiomyopathy [43]. A reduced single mitochondrion ATP flux may limit sarcomere contraction, leading to a compensatory proliferation of the cardiac mitochondria, while the myocardium may continue to contract inefficiently and dyssynchronously due to its adaptation, as previously anticipated [5, 44]. Notably, the cardiac guanine-to-adenine nucleotides ratio was amplified, likely as a compensatory mechanism to fewer adenine nucleotides. This was in agreement with a

previous finding of a higher concentration of guanine nucleotides in human hearts with dilated and hypertrophic cardiomyopathy [45]. It is well known that guanine nucleotides are an essential component of G-protein signalling, with links to the adenylate cyclase machinery, and so changes in their concentration may impair regulatory mechanisms in the heart [46].

It is also well established that the major source of ATP regeneration is the creatine kinase system [47]. Depletion of the phosphocreatine (PCr) concentration is a typical feature of heart failure and has been described in many different animal models of cardiomyopathy [48, 49]. A reduced PCr concentration, and PCr/Cr ratio, is other cardiac energy metabolism parameters that we found to be deregulated in HD settings. A decreased PCr/Cr ratio directly translates into lower values of phosphorylation potential, leading to a decreased cardiac muscle contraction and an impaired heart rate as previously described in HD mouse models [5].

To examine the steady-state internal redox status in HD hearts, we assessed the levels of oxidized and reduced forms of nicotinamide adenine dinucleotides – NAD+ and NADH. We demonstrated a reduced NADH level and NADH/NAD+ ratio in the mouse models. This may be an indication of redox imbalance, and could suggest an inherent dysfunction of mitochondria, or be indicative of alterations in a mitochondrial function upstream of oxidative phosphorylation [50]. In particular, this could indicate a disrupted efficiency of the Krebs cycle. Further studies should be done to identify whether this is caused by enzyme inhibition or down-regulation, or whether there is insufficient supply of acetyl-CoA or anaplerotic substrates.

The cardiac energy metabolism and steady state internal redox imbalance, found in both symptomatic HD mouse models, may activate energy regenerating pathways like AMP-activated protein kinase (AMPK) phosphorylation. AMPK is a heterotrimeric complex kinase comprising a catalytic subunit (α-subunit) and two regulatory subunits (β- and γ-subunits). Both α- and β-subunits form two isoforms, $\alpha 1$, $\alpha 2$ and $\beta 1$, $\beta 2$, while the γ-subunit is present in three $\gamma 1$, $\gamma 2$, and $\gamma 3$ isoforms [22]. The α-subunit contains the catalytic domain of the serine/threonine protein kinase (Thr^{172}) whose phosphorylation is crucial for AMPK activation [51]. We found that AMPK was hyperphosphorylated in HD mouse model hearts. It is known that AMPK plays an important role in ATP regeneration by the cellular uptake of glucose, β-oxidation of fatty acids and regulation of mitochondrial biogenesis [52]. It is likely that an enhanced AMPK activity results in a cardiac substrate preference shift in symptomatic HD animals, as was demonstrated by decreased ^{13}C glutamate enrichment and a reduced ratio of [^{13}C glutamate] to [^{13}C alanine] in HD mouse model hearts.

Similarly, a reduced glucose oxidative metabolism was observed both in skeletal muscle in HD mouse models [14] and in the cardiac mitochondria obtained from patients with a dilated cardiomyopathy [12]. A decreased glucose metabolism could be the cause or result of lower transcript levels of *Hk2* (Hexokinase 2; an enzyme that phosphorylates glucose). Hexokinase activity is the initiating step for virtually all glucose utilization pathways observed in HD mouse model hearts. Moreover, there are some data suggesting that a reduction in hexokinase 2 levels might result in a decreased cardiac function and altered remodelling of the heart, in ischemia-reperfusion, by increasing cell death, fibrosis and reducing angiogenesis in cardiomyocytes [53].

No significant changes in transcripts of molecules involved in the metabolism of fatty acids such as *Ppargc1a* (Peroxisome proliferator-activated receptor gamma coactivator 1-alpha) and *Ppara* (Peroxisome proliferator-activated receptor alpha) were identified. Thus, one may conclude that the myocardium failure in HD could be caused by alterations in specific energy substrate metabolism [54]. In particular, a failing heart typically shifts metabolism from carbohydrate oxidation towards metabolism of fatty acids, which may cause a decline in contractile function and intensify the progression of pump failure [53]. Thus, such observed shifts determine reductions in myocardial oxygen consumption efficiency and we observed this phenomenon in HD hearts. Although the protective AMPK pathway was not properly activated, as judged on the lack of ATP regeneration, it is likely that mutant HTT can exert loss or gain of function effects on mitochondrial enzymes. Alternatively, in HD there could be a lack of trophic signals from the CNS [5, 55] that may lead to impairment of proteins involved in energy metabolism.

Despite the fact that there is no global transcriptional deregulation in hearts, in either HD mouse model [5], we found a significant down-regulation of genes involved in purine *de novo* biosynthesis, such as *Adsl, Adlssl1, Gart,* and in reconversion of adenine nucleotides, like *Gmps* and *Akt1*. Interestingly, it is well established that an induction of genes involved in *de novo* purine nucleotide synthesis is observed in cardiac hypertrophy in rats [56]. Our findings are in line with a previous study showing a substantial acceleration of purine synthesis and turnover in $HTT^{-/-}$ murine embryonic stem cells, likely due to increased purine biosynthesis [57]. It is possible that reduced purine synthesis and re-conversion of adenine nucleotides led to the changes in catabolism of nucleotides that we observed in HD mouse models. Indeed, we found a number of adenosine catabolites such as inosine, hypoxanthine, xanthine, uridine or uric acid at increased levels in the sera of the HD murine models. More importantly, uridine and hypoxanthine levels were also found to be increased in the plasma of

symptomatic HD patients. Hence, for the first time, our study identified biomarkers that might be linked to HD progression both in pre-clinical and clinical settings.

It is likely that the catabolites that we we observed in sera were released by the affected heart and/or skeletal muscle tissues. In fact we showed that these catabolites were accumulated within the heart mass in the R6/2 mouse model [58]. In addition, these findings are supported by the observation of the up-regulation of genes involved in the adenosine degradation pathway, such as *Ada* or *Dpp4*. Adenosine is known to be a protective agent in ischemic heart failure [59] and administration of adenosine metabolism inhibitors results in an improvement of cardiac function [60]. Moreover, it is well known that polymorphisms within the *Ada* gene can predispose to chronic heart failure [61]. Altered transcripts of genes responsible for ATP degradation, such as *Entpd2* (Ectonucleoside triphosphate diphosphohydrolase 2) and *Nme3* (Nucleoside diphosphate kinase 3), were observed in the *Hdh*Q150 mouse model and could interfere with regulation of the ATP pool. *Entpd2* has been identified as a key enzyme with a role in regulating nucleotide-mediated signaling, and in controlling the rate, amount and timing of nucleotide degradation [62]. It is well-established that nucleoside diphosphate kinase possesses a histidine kinase activity for G-beta proteins that could potentially contribute to receptor-independent regulation of cAMP synthesis and the contractility of cardiomyocytes [63]. Nonetheless, no changes were observed in the transcript levels of genes involved in nucleotide catabolite pathways, such as guanine, inosine or hypoxanthine degradation. Therefore down-regulation of synthesis of adenine nucleotides, and changes in their catabolism, may intensify the deterioration in energy equilibrium.

5. CONCLUSIONS

In summary, HD mouse models develop a notable decrease in cardiac energy metabolism, concomitant with AMPK hyperphosphorylation. This may contribute to a shift in cardiac substrate preference that is accompanied by decreased oxidation and lack of ATP regeneration, leading to the accumulation of nucleotide catabolites in sera, both in HD mice and in HD clinical samples (Fig. 8). In addition, cardiac transcriptional dysregulation of genes occurs, involving processes such as purine biosynthesis and catabolism of adenine nucleotides, which may in turn activate the development of pathological features leading to HD-related cardiomyopathy One may conclude that the energy imbalance and altered metabolism of nucleotides is likely to be a contributor to the apparent contractile heart dysfunction that has been previously reported in HD mouse models [5].

Our data strongly suggest that there is value in embarking on the development of new therapies to improve energy metabolism in HD affected hearts. Likely candidates would include inhibitors of mitochondrial permeability transition pore (mPTP) opening and compounds in clinical trials, such as CoQ10 and creatine [64]. Other candidates would include substances that provide anaplerotic substrates for the Krebs cycle, such as branched-chain amino acids (BCAA) - whose concentrations have been found to be decreased in HD patients' plasma; reviewed in [65].

Alternatively, PPAR activators are already widely-used in pre-clinical trials [64]. These small molecule drugs promote the expression of genes that enhance energy production and optimize the quality control of proteins and organelles. Moreover, Dickey and colleagues recently tested the PPARδ agonist KD3010 in HD N171-82Q transgenic mice. They observed improved motor function, decreased neurodegeneration and longer survival in HD mice [66]. Based on these promising results it would be of interest to evaluate how PPAR activation might improve the energy metabolism of other tissues affected in HD.

Finally, a different therapeutic strategy may include testing molecules to improve the metabolism of nucleotides directly. Our previous studies identified that a combined treatment of cardiomyocytes with adenosine metabolism inhibitors and substrates for nucleotide synthesis resulted in improvements in cardiac mechanical function, in the energy status and of the adenine nucleotide pool [67, 68]. Ultimately, this therapeutic avenue that may well be amenable to small molecule therapeutics and may even be widely applicable to other neurodegenerative diseases.

6. ACKNOWLEDGEMENT

This work was supported by the National Science Centre of Poland (2011/01/B/NZ4/03719) and (2015/17/N/NZ4/028410); Foundation for Polish Science (TEAM/2011-8/7), and funding from European Research Council grant H2020 - ERC-2014-PoC 641232 - Fingers4Cure. These funders had no role in study design, data collection and analysis, decision to publish or preparation of the manuscript.

7. CONFLICTS OF INTEREST STATEMENT

None declared.

REFERENCES

[1] D. Zielonka, M. Mielcarek, G.B. Landwehrmeyer, Update on Huntington's disease: advances in care and emerging therapeutic options, Parkinsonism Relat Disord, 21 (2015) 169-178.
[2] S.H. Li, G. Schilling, W.S. Young, 3rd, X.J. Li, R.L. Margolis, O.C. Stine, M.V. Wagster, M.H. Abbott, M.L. Franz, N.G. Ranen, et al., Huntington's disease gene (IT15) is widely expressed in human and rat tissues, Neuron, 11 (1993) 985-993.
[3] S.W. Davies, M. Turmaine, B.A. Cozens, M. DiFiglia, A.H. Sharp, C.A. Ross, E. Scherzinger, E.E. Wanker, L. Mangiarini, G.P. Bates, Formation of neuronal intranuclear inclusions underlies the neurological dysfunction in mice transgenic for the HD mutation, Cell, 90 (1997) 537-548.
[4] H. Moffitt, G.D. McPhail, B. Woodman, C. Hobbs, G.P. Bates, Formation of polyglutamine inclusions in a wide range of non-CNS tissues in the HdhQ150 knock-in mouse model of Huntington's disease, PLoS One, 4 (2009) e8025.
[5] M. Mielcarek, L. Inuabasi, M.K. Bondulich, T. Muller, G.F. Osborne, S.A. Franklin, D.L. Smith, A. Neueder, J. Rosinski, I. Rattray, A. Protti, G.P. Bates, Dysfunction of the CNS-heart axis in mouse models of Huntington's disease, PLoS Genet, 10 (2014) e1004550.
[6] P. Harjes, E.E. Wanker, The hunt for huntingtin function: interaction partners tell many different stories, Trends Biochem Sci, 28 (2003) 425-433.
[7] D. Zielonka, I. Piotrowska, M. Mielcarek, Cardiac dysfunction in Huntington's Disease., Exp Clin Cardiol, 20 (2014) 2547-2554.
[8] C. Stephen, S. Hersch, H. Rosas, Huntington’s disease and the heart: Electrocardiogram abnormalities suggest cardiac involvement., Neurology, 84 (2016).
[9] M. Mielcarek, M.K. Bondulich, L. Inuabasi, S.A. Franklin, T. Muller, G.P. Bates, The Huntington's disease-related cardiomyopathy prevents a hypertrophic response in the R6/2 mouse model, PLoS One, 9 (2014) e108961.
[10] A.M. Walters, G.A. Porter, Jr., P.S. Brookes, Mitochondria as a drug target in ischemic heart disease and cardiomyopathy, Circ Res, 111 (2012) 1222-1236.
[11] J. Finsterer, S. Kothari, Cardiac manifestations of primary mitochondrial disorders, Int J Cardiol, 177 (2014) 754-763.
[12] E. Rosello-Lleti, E. Tarazon, M.G. Barderas, A. Ortega, M. Otero, M.M. Molina-Navarro, F. Lago, J.R. Gonzalez-Juanatey, A. Salvador, M. Portoles, M. Rivera, Heart mitochondrial proteome study elucidates changes in cardiac energy metabolism and antioxidant PRDX3 in human dilated cardiomyopathy, PLoS One, 9 (2014) e112971.
[13] S.C. Kolwicz, Jr., S. Purohit, R. Tian, Cardiac metabolism and its interactions with contraction, growth, and survival of cardiomyocytes, Circ Res, 113 (2013) 603-616.
[14] M. Mielcarek, M. Toczek, C.J. Smeets, S.A. Franklin, M.K. Bondulich, N. Jolinon, T. Muller, M. Ahmed, J.R. Dick, I. Piotrowska, L. Greensmith, R.T. Smolenski, G.P. Bates, HDAC4-myogenin axis as an important marker of HD-related skeletal muscle atrophy, PLoS Genet, 11 (2015) e1005021.
[15] R.T. Smolenski, D.R. Lachno, S.J. Ledingham, M.H. Yacoub, Determination of sixteen nucleotides, nucleosides and bases using high-performance liquid chromatography and its application to the study of purine metabolism in hearts for transplantation, Journal of chromatography, 527 (1990) 414-420.
[16] G.K. Soppa, R.T. Smolenski, N. Latif, A.H. Yuen, A. Malik, J. Karbowska, Z. Kochan, C.M. Terracciano, M.H. Yacoub, Effects of chronic administration of clenbuterol on function and metabolism of adult rat cardiac muscle, American journal of physiology. Heart and circulatory physiology, 288 (2005) H1468-1476.
[17] M. Mielcarek, C.L. Benn, S.A. Franklin, D.L. Smith, B. Woodman, P.A. Marks, G.P. Bates, SAHA decreases HDAC 2 and 4 levels in vivo and improves molecular phenotypes in the R6/2 mouse model of Huntington's disease, PLoS One, 6 (2011) e27746.

[18] L. Mangiarini, K. Sathasivam, M. Seller, B. Cozens, A. Harper, C. Hetherington, M. Lawton, Y. Trottier, H. Lehrach, S.W. Davies, G.P. Bates, Exon 1 of the HD gene with an expanded CAG repeat is sufficient to cause a progressive neurological phenotype in transgenic mice, Cell, 87 (1996) 493-506.
[19] C.H. Lin, S. Tallaksen-Greene, W.M. Chien, J.A. Cearley, W.S. Jackson, A.B. Crouse, S. Ren, X.J. Li, R.L. Albin, P.J. Detloff, Neurological abnormalities in a knock-in mouse model of Huntington's disease, Hum Mol Genet, 10 (2001) 137-144.
[20] M.J. McLeish, G.L. Kenyon, Relating structure to mechanism in creatine kinase, Crit Rev Biochem Mol Biol, 40 (2005) 1-20.
[21] S. Burakowski, R.T. Smolenski, J. Bellwon, A. Kubasik, D. Ciecwierz, A. Rynkiewicz, Exercise stress test and comparison of ST change with cardiac nucleotide catabolite production in patients with coronary artery disease, Cardiol J, 14 (2007) 573-579.
[22] D.G. Hardie, AMP-activated protein kinase: an energy sensor that regulates all aspects of cell function, Genes Dev, 25 (2011) 1895-1908.
[23] D. Armenta-Medina, L. Segovia, E. Perez-Rueda, Comparative genomics of nucleotide metabolism: a tour to the past of the three cellular domains of life, BMC Genomics, 15 (2014) 800.
[24] Y. Natsumeda, N. Prajda, J.P. Donohue, J.L. Glover, G. Weber, Enzymic capacities of purine de Novo and salvage pathways for nucleotide synthesis in normal and neoplastic tissues, Cancer Res, 44 (1984) 2475-2479.
[25] A. Bouhss, H. Sakamoto, N. Palibroda, M. Chiriac, R. Sarfati, J.M. Smith, C.T. Craescu, O. Barzu, Enzymatic synthesis of guanine nucleotides labeled with 15N at the 2-amino group of the purine ring, Anal Biochem, 225 (1995) 18-23.
[26] F. Carlucci, A. Tabucchi, R. Pagani, E. Marinello, Synthesis of adenine and guanine nucleotides at the 'inosinic branch point' in lymphocytes of leukemia patients, Biochim Biophys Acta, 1454 (1999) 106-114.
[27] P. Dzeja, A. Terzic, Adenylate kinase and AMP signaling networks: metabolic monitoring, signal communication and body energy sensing, International journal of molecular sciences, 10 (2009) 1729-1772.
[28] B. Kutryb-Zajac, P. Zukowska, M. Toczek, M. Zabielska, M. Lipinski, I. Rybakowska, S. Chlopicki, E.M. Slominska, R.T. Smolenski, Extracellular nucleotide catabolism in aortoiliac bifurcation of atherosclerotic ApoE/LDLr double knock out mice, Nucleosides, nucleotides & nucleic acids, 33 (2014) 323-328.
[29] E. Matteucci, O. Giampietro, Dipeptidyl peptidase-4 (CD26): knowing the function before inhibiting the enzyme, Current medicinal chemistry, 16 (2009) 2943-2951.
[30] M. Toczek, B. Kutryb-Zajac, M. Kapczynska, M. Lipinski, E.M. Slominska, R.T. Smolenski, Extracellular adenine nucleotide catabolism in heart valves, Nucleosides, nucleotides & nucleic acids, 33 (2014) 329-332.
[31] S. Lutz, R. Mura, D. Baltus, M. Movsesian, W. Kubler, F. Niroomand, Increased activity of membrane-associated nucleoside diphosphate kinase and inhibition of cAMP synthesis in failing human myocardium, Cardiovascular research, 49 (2001) 48-55.
[32] P.L. Walker, A. Corrigan, M. Arenas, E. Escuredo, L. Fairbanks, A. Marinaki, Purine nucleoside phosphorylase deficiency: a mutation update, Nucleosides, nucleotides & nucleic acids, 30 (2011) 1243-1247.
[33] J. Yang, K. Kamide, Y. Kokubo, S. Takiuchi, T. Horio, T. Matayoshi, H. Yasuda, Y. Miwa, M. Yoshii, F. Yoshihara, S. Nakamura, H. Nakahama, H. Tomoike, T. Miyata, Y. Kawano, Associations of hypertension and its complications with variations in the xanthine dehydrogenase gene, Hypertension research : official journal of the Japanese Society of Hypertension, 31 (2008) 931-940.
[34] D.J. Roberts, S. Miyamoto, Hexokinase II integrates energy metabolism and cellular protection: Akting on mitochondria and TORCing to autophagy, Cell Death Differ, 22 (2015) 248-257.

[35] D. Zielonka, I. Piotrowska, J.T. Marcinkowski, M. Mielcarek, Skeletal muscle pathology in Huntington's disease, Front Physiol, 5 (2014) 380.
[36] M.J. Mihm, D.M. Amann, B.L. Schanbacher, R.A. Altschuld, J.A. Bauer, K.R. Hoyt, Cardiac dysfunction in the R6/2 mouse model of Huntington's disease, Neurobiology of disease, 25 (2007) 297-308.
[37] H. Kiriazis, N.L. Jennings, P. Davern, G. Lambert, Y. Su, T. Pang, X. Du, L. La Greca, G.A. Head, A.J. Hannan, X.J. Du, Neurocardiac dysregulation and neurogenic arrhythmias in a transgenic mouse model of Huntington's disease, J Physiol, 590 (2012) 5845-5860.
[38] B.T. Wu, M.C. Chiang, C.Y. Tasi, C.H. Kuo, W.C. Shyu, C.L. Kao, C.Y. Huang, S.D. Lee, Cardiac Fas-Dependent and Mitochondria-Dependent Apoptotic Pathways in a Transgenic Mouse Model of Huntington's Disease, Cardiovascular toxicology, (2015).
[39] M. Mielcarek, M. Isalan, A shared mechanism of muscle wasting in cancer and Huntington's disease, Clin Transl Med, 4 (2015) 34.
[40] C. Saft, J. Zange, J. Andrich, K. Muller, K. Lindenberg, B. Landwehrmeyer, M. Vorgerd, P.H. Kraus, H. Przuntek, L. Schols, Mitochondrial impairment in patients and asymptomatic mutation carriers of Huntington's disease, Mov Disord, 20 (2005) 674-679.
[41] A. Ciammola, J. Sassone, L. Alberti, G. Meola, E. Mancinelli, M.A. Russo, F. Squitieri, V. Silani, Increased apoptosis, Huntingtin inclusions and altered differentiation in muscle cell cultures from Huntington's disease subjects, Cell Death Differ, 13 (2006) 2068-2078.
[42] M.A. Conway, J. Allis, R. Ouwerkerk, T. Niioka, B. Rajagopalan, G.K. Radda, Detection of low phosphocreatine to ATP ratio in failing hypertrophied human myocardium by 31P magnetic resonance spectroscopy, Lancet, 338 (1991) 973-976.
[43] R.C. Starling, D.F. Hammer, R.A. Altschuld, Human myocardial ATP content and in vivo contractile function, Molecular and cellular biochemistry, 180 (1998) 171-177.
[44] K.A. Strauss, L. DuBiner, M. Simon, M. Zaragoza, P.P. Sengupta, P. Li, N. Narula, S. Dreike, J. Platt, V. Procaccio, X.R. Ortiz-Gonzalez, E.G. Puffenberger, R.I. Kelley, D.H. Morton, J. Narula, D.C. Wallace, Severity of cardiomyopathy associated with adenine nucleotide translocator-1 deficiency correlates with mtDNA haplogroup, Proc Natl Acad Sci U S A, 110 (2013) 3453-3458.
[45] K.K. Kalsi, R.T. Smolenski, R.D. Pritchard, A. Khaghani, A.M. Seymour, M.H. Yacoub, Energetics and function of the failing human heart with dilated or hypertrophic cardiomyopathy, European journal of clinical investigation, 29 (1999) 469-477.
[46] J.W. Fleming, P.L. Wisler, A.M. Watanabe, Signal transduction by G proteins in cardiac tissues, Circulation, 85 (1992) 420-433.
[47] L. Guimaraes-Ferreira, Role of the phosphocreatine system on energetic homeostasis in skeletal and cardiac muscles, Einstein, 12 (2014) 126-131.
[48] L. Nascimben, J. Friedrich, R. Liao, P. Pauletto, A.C. Pessina, J.S. Ingwall, Enalapril treatment increases cardiac performance and energy reserve via the creatine kinase reaction in myocardium of Syrian myopathic hamsters with advanced heart failure, Circulation, 91 (1995) 1824-1833.
[49] M. Spindler, K.W. Saupe, M.E. Christe, H.L. Sweeney, C.E. Seidman, J.G. Seidman, J.S. Ingwall, Diastolic dysfunction and altered energetics in the alphaMHC403/+ mouse model of familial hypertrophic cardiomyopathy, The Journal of clinical investigation, 101 (1998) 1775-1783.
[50] I.L. Ferreira, T. Cunha-Oliveira, M.V. Nascimento, M. Ribeiro, M.T. Proenca, C. Januario, C.R. Oliveira, A.C. Rego, Bioenergetic dysfunction in Huntington's disease human cybrids, Experimental neurology, 231 (2011) 127-134.
[51] T.T. Kim, J.R. Dyck, Is AMPK the savior of the failing heart?, Trends in endocrinology and metabolism: TEM, 26 (2015) 40-48.
[52] M. Suter, U. Riek, R. Tuerk, U. Schlattner, T. Wallimann, D. Neumann, Dissecting the role of 5'-AMP for allosteric stimulation, activation, and deactivation of AMP-activated protein kinase, J Biol Chem, 281 (2006) 32207-32216.

[53] R. Wu, K.M. Smeele, E. Wyatt, Y. Ichikawa, O. Eerbeek, L. Sun, K. Chawla, M.W. Hollmann, V. Nagpal, S. Heikkinen, M. Laakso, K. Jujo, J.A. Wasserstrom, C.J. Zuurbier, H. Ardehali, Reduction in hexokinase II levels results in decreased cardiac function and altered remodeling after ischemia/reperfusion injury, Circ Res, 108 (2011) 60-69.
[54] I.F. Kodde, J. van der Stok, R.T. Smolenski, J.W. de Jong, Metabolic and genetic regulation of cardiac energy substrate preference, Comparative biochemistry and physiology. Part A, Molecular & integrative physiology, 146 (2007) 26-39.
[55] M. Mielcarek, Huntington's disease is a multi-system disorder, Rare diseases, 3 (2015) e1058464.
[56] Y. Liu, X. Yan, G. Mao, L. Fang, B. Zhao, Y. Liu, H. Tang, N. Wang, Metabonomic profiling revealed an alteration in purine nucleotide metabolism associated with cardiac hypertrophy in rats treated with thiazolidinediones, J Proteome Res, 12 (2013) 5634-5641.
[57] I. Ismailoglu, Q. Chen, M. Popowski, L. Yang, S.S. Gross, A.H. Brivanlou, Huntingtin protein is essential for mitochondrial metabolism, bioenergetics and structure in murine embryonic stem cells, Developmental biology, 391 (2014) 230-240.
[58] M. Toczek, B. Kutryb-Zajac, P. Zukowska, E. Slominska, M. Isalan, M. Mielcarek, R.T. Smolenski, CHANGES IN CARDIAC NUCLEOTIDE METABOLISM IN HUNTINGTON'S DISEASE Nucleosides, nucleotides & nucleic acids, in press (2016).
[59] J.P. Headrick, K.J. Ashton, R.B. Rose'meyer, J.N. Peart, Cardiovascular adenosine receptors: expression, actions and interactions, Pharmacology & therapeutics, 140 (2013) 92-111.
[60] R.T. Smolenski, O. Raisky, E.M. Slominska, H. Abunasra, K.K. Kalsi, J. Jayakumar, K. Suzuki, M.H. Yacoub, Protection from reperfusion injury after cardiac transplantation by inhibition of adenosine metabolism and nucleotide precursor supply, Circulation, 104 (2001) I246-252.
[61] H.R. He, Y.J. Li, G.H. He, Y.J. Wang, Y.J. Zhai, J. Xie, W.P. Zhang, Y.L. Dong, J. Lu, The adenosine deaminase gene polymorphism is associated with chronic heart failure risk in Chinese, International journal of molecular sciences, 15 (2014) 15259-15271.
[62] B. Rucker, M.E. Almeida, T.A. Libermann, L.F. Zerbini, M.R. Wink, J.J. Sarkis, E-NTPDases and ecto-5'-nucleotidase expression profile in rat heart left ventricle and the extracellular nucleotide hydrolysis by their nerve terminal endings, Life sciences, 82 (2008) 477-486.
[63] H.J. Hippe, M. Luedde, S. Lutz, H. Koehler, T. Eschenhagen, N. Frey, H.A. Katus, T. Wieland, F. Niroomand, Regulation of cardiac cAMP synthesis and contractility by nucleoside diphosphate kinase B/G protein beta gamma dimer complexes, Circ Res, 100 (2007) 1191-1199.
[64] F. Mochel, P. Charles, F. Seguin, J. Barritault, C. Coussieu, L. Perin, Y. Le Bouc, C. Gervais, G. Carcelain, A. Vassault, J. Feingold, D. Rabier, A. Durr, Early energy deficit in Huntington disease: identification of a plasma biomarker traceable during disease progression, PLoS One, 2 (2007) e647.
[65] W. Duan, M. Jiang, J. Jin, Metabolism in HD: still a relevant mechanism?, Mov Disord, 29 (2014) 1366-1374.
[66] A.S. Dickey, V.V. Pineda, T. Tsunemi, P.P. Liu, H.C. Miranda, S.K. Gilmore-Hall, N. Lomas, K.R. Sampat, A. Buttgereit, M.J. Torres, A.L. Flores, M. Arreola, N. Arbez, S.S. Akimov, T. Gaasterland, E.R. Lazarowski, C.A. Ross, G.W. Yeo, B.L. Sopher, G.K. Magnuson, A.B. Pinkerton, E. Masliah, A.R. La Spada, PPAR-delta is repressed in Huntington's disease, is required for normal neuronal function and can be targeted therapeutically, Nature medicine, 22 (2016) 37-45.
[67] R.T. Smolenski, K.K. Kalsi, M. Zych, Z. Kochan, M.H. Yacoub, Adenine/ribose supply increases adenosine production and protects ATP pool in adenosine kinase-inhibited cardiac cells, Journal of molecular and cellular cardiology, 30 (1998) 673-683.

[68] R.T. Smolenski, O. Raisky, E.M. Slominska, H. Abunasra, K.K. Kalsi, J. Jayakumar, K. Suzuki, M.H. Yacoub, Protection from reperfusion injury after cardiac transplantation by inhibition of adenosine metabolism and nucleotide precursor supply, Circulation, 104 (2001) I246-I252.

LEGENDS TO FIGURES

Figure 1. Adenine nucleotides, phosphocreatine and creatine levels in symptomatic HD mouse model hearts. (A) ATP and ADP **(B)** levels in wild-type, R6/2 and *Hdh*Q150 mice. **(C)** AMP level. **(D)** The ATP/ADP ratio. **(E)** Phosphocreatine and creatine levels. **(F)** The PCr/Cr ratio. Data presented as mean ± SEM; n=5; * $p<0.05$, ** $p<0.01$.

Figure 2. Total levels of adenine and guanine nucleotides, and NAD+ or NADH levels in HD mouse model hearts. (A) The total concentration of adenine nucleotides in wild-type, R6/2 and *Hdh*Q150 mouse hearts. **(B)** The total concentration of guanine nucleotides. **(C)** Guanine/adenine nucleotides ratio. **(D)** NAD+ and NADH levels **(E)**. **F.** NADH/NAD+ ratio. Data presented as mean ± SEM; n=5; * $p<0.05$.

Figure 3. Intensive increases of adenine nucleotide catabolites and uridine concentration in the sera of HD mouse models. (A) Inosine, hypoxanthine, xanthine and uric acid levels in wild-type, R6/2 and *Hdh*Q150 mouse serum. **(B)** Uridine concentration. Data presented as mean ± SEM; n=5; ** $p<0.01$, *** $p<0.001$.

Figure 4. Concentrations of uric acid, hypoxanthine and uridine in the plasma of HD patients. (A) Uric acid level. **(B)** Hypoxanthine concentration. **(C)** Linear regression of mutant CAG repeat length and hypoxanthine concentration. **(D)** Linear regression of HD disease burden and hypoxanthine concentration. **(E)** Uridine concentration. **(F)** Linear regression of uridine levels and mutant CAG repeat length. **(G)** Linear regression of uridine concentration and HD disease burden. Data presented as mean ± SEM; n=5; * $p<0.05$; *** $p<0.001$.

Figure 5. Changes in the cardiac substrate preference and AMP-regulated protein kinase phosphorylation level in HD mouse models. (A) ^{13}C glutamate / ^{13}C glucose ratio in the blood of wild-type, R6/2 and *Hdh*Q150 mice. **(B)** ^{13}C alanine / ^{13}C glucose ratios in the blood of HD mouse models. **(C)** ^{13}C glutamate / ^{13}C alanine ratio in the hearts of HD mouse models **(D).** The AMPK phosphorylation level in the hearts of HD mouse models. Data presented as mean ± SEM; n=5; * $p<0.05$; *** $p<0.001$.

Figure 6. Transcriptional remodeling of genes involved in synthesis of nucleotides. (A) Transcripts of genes involved in *de novo* purine biosynthesis (*Adsl (*Adenylosuccinate lyase*), Adlssl1 (*Adenylosuccinate lyase 1), *Gart* (Phosphoribosylglycinamide formyltransferase), *Ppart (*Phosphoribosyl pyrophosphate amidotransferase*), Prpsap2 (*Phosphoribosyl

pyrophosphate synthetase-associated protein 2)) and the purine nucleotide salvage pathway (*Aprt (*Adenine phosphoribosyltransferase)). **(B)** Transcripts of genes involved in conversion of adenine nucleotides (*Ak1* (Adenylate kinase 1), *Gmpr* (Guanosine monophosphate reductase), *Gmps* (Guanosine monophosphate synthetase) and *Impdh2* (inosine monophosphate dehydrogenase 2)). All Taqman qPCR values were normalized to the geometric mean of three housekeeping genes: *Actb*, *Cyc1* and *Gapdh*. Error bars are ± SEM (n = 5). Student's *t*-test: **p*<0.05, ***p*<0.01; ****p*<0.001.

Figure 7. Transcriptional remodeling of genes involved in catabolism of nucleotides and substrate metabolism. (A) Transcripts of genes involved in adenosine metabolism (*Ada (*Adenosine deaminase), *Adk* (Adenosine kinase), *Dpp4* (Dipeptydyl peptidase-4) and *Nt5e* (Ecto-5'-nucelotidase)). **(B)** Transcript levels of genes involved in adenine nucleotide metabolism (*Ampd3* (Adenosine deaminase 3), *Entpd2* (Ectonucleoside triphosphate diphosphohydrolase 2) *Nme1* (Nucleoside diphosphate kinase 1), *Nme2* (Nucleoside diphosphate kinase 2) and *Nme3* (Nucleoside diphosphate kinase 3)). **(C)** Transcripts of genes involved in guanine (*Gda* (Guanine deaminase)), inosine (*Pnp* (Purine nucleoside phosphorylase)) and hypoxanthine (*Xdh* (Xanthine dehydrogenase)) degradation pathways. **(D)** Transcripts of genes involved in glucose (*Hk2* (Hexokinase 2)), fatty acids (*Ppargc1a* (Peroxisome proliferator-activated receptor gamma coactivator 1-alpha) and *Ppara* (Peroxisome proliferator-activated receptor alpha) and energy (*Prkaa1* (AMP- activated protein kinase)) metabolism. All Taqman qPCR values were normalized to the geometric mean of three housekeeping genes: *Actb*, *Cyc1* and *Gapdh*. Error bars are ± SEM (n = 5). Student's *t*-test: **p*<0.05, ***p*<0.01,****p*<0.001.

Figure 8. A model depicting the mechanism by which cardiac mitochondriopathy may induce HD-related cardiomyopathy. ***Mitochondria:*** the HD-related cardiac impairment of energetic functions is a result of alterations in the flux of the Krebs cycle, as indicated by a decreased ratio of [^{13}C glutamate] to [^{13}C alanine], and a reduced NADH/NAD+ ratio. ***HD cardiac cell:*** the reduced NADH/NAD+ ratio leads to diminished cardiac ATP and PCr concentrations, as well as decreased ATP/ADP, and an increased AMP concentration. The increased AMP level leads to activation of AMPK. However, AMPK is unable to restore cellular energy homeostasis. ***Transcription:*** Possibly due to the changes in energy metabolism, the cardiomyocytes of HD mice were also characterized by the transcriptional remodelling of genes involved in nucleotide pool regulation (down-regulation of *Adsl*, *Adssl1*, *Gart*, *Gmps*, *Ak1*, *Entpd2*, *Nme3* and up-regulation of *Gmpr*, *Ada*, *Dpp-4*, *Prkaa1*).

These alterations may contribute to a reduction in the cardiac adenine nucleotide pool and alterations in guanine/adenine nucleotides ratio. ***Plasma/serum:*** the impaired nucleotide and energy metabolism results in the increased production of catabolites of adenine nucleotides (inosine, hypoxanthine, xanthine and uric acid) and pyrimidines (uridine) and these are found at elevated concentrations in the sera of HD mouse models. Interestingly, elevated levels of uridine and hypoxanthine were also found in plasma from HD patients and were correlated with HD progression.

ABBREVIATIONS

HD - Huntington's disease; *HTT* - huntingtin gene; EDL – Extensor digitorum longus muscle; ATP - adenosine triphosphate, ADP - adenosine diphosphate; AMP - adenosine monophosphate; Cr – creatine; PCr – phosphocreatine; PCr/Cr ratio – phosphocreatine/ creatine ratio; NAD+ - oxidized nicotinamide adenine dinucleotides; NADH - reduced nicotinamide adenine dinucleotides; AMPK - AMP-activated protein kinase; qPCR – quantitative polymerase chain reaction; *Ada* - Adenosine deaminase; *Adk* - Adenosine kinase; *Dpp4* - Dipeptydyl peptidase-4; *Nt5e* - Ecto-5'-nucelotidase; *Ampd3* - Adenosine deaminase 3; *Entpd2* - Ectonucleoside triphosphate diphosphohydrolase 2; *Nme1* - Nucleoside diphosphate kinase 1; *Nme2* - Nucleoside diphosphate kinase 2; *Nme3* - Nucleoside diphosphate kinase 3; *Gda* - Guanine deaminase inosine ; *Pnp* - Purine nucleoside phosphorylase; *Xdh* - Xanthine dehydrogenase; *Hk2* - Hexokinase 2; *Ppargc1a* - Peroxisome proliferator-activated receptor gamma coactivator 1-alpha; *Ppara* - Peroxisome proliferator-activated receptor alpha; *Adsl* - Adenylosuccinate lyase; *Adlssl1* - Adenylosuccinate lyase 1; *Gart* - Phosphoribosylglycinamide formyltransferase; *Ppart* - Phosphoribosyl pyrophosphate amidotransferase; *Prpsap2* - Phosphoribosyl pyrophosphate synthetase-associated protein 2; *Aprt* - Adenine phosphoribosyltransferase; *Ak1* - Adenylate kinase 1; *Gmpr* - Guanosine monophosphate reductase; *Gmps* - Guanosine monophosphate synthetase; *Impdh2* - inosine monophosphate dehydrogenase 2

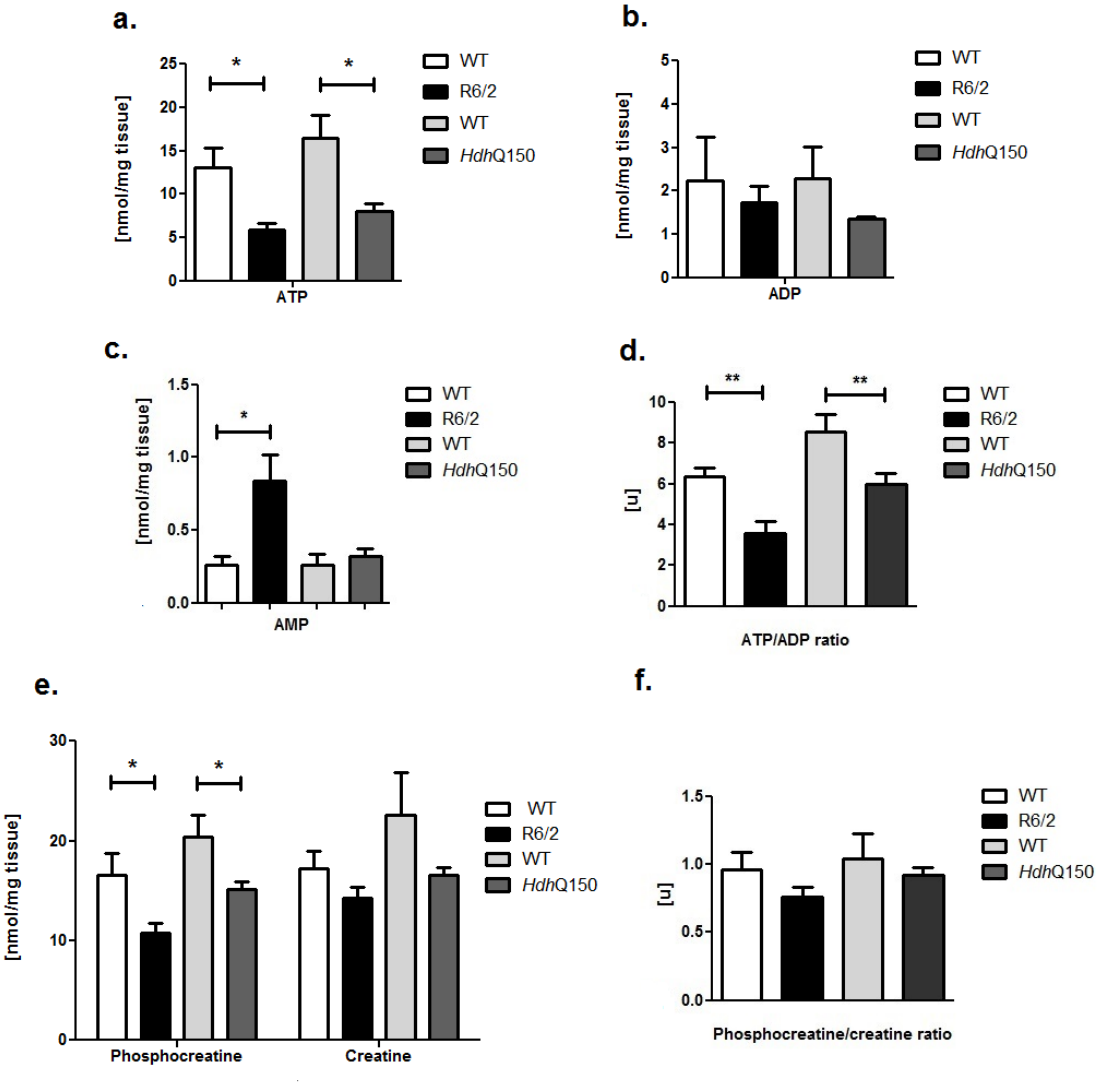

a.
[nmol/mg tissue]
ATP
WT
R6/2
WT
HdhQ150
b.
[nmol/mg tissue]
ADP
c.
[nmol/mg tissue]
AMP
d.
[u]
ATP/ADP ratio
e.
[nmol/mg tissue]
Phosphocreatine
Creatine
f.
[u]
Phosphocreatine/creatine ratio

Figure 1

Figure

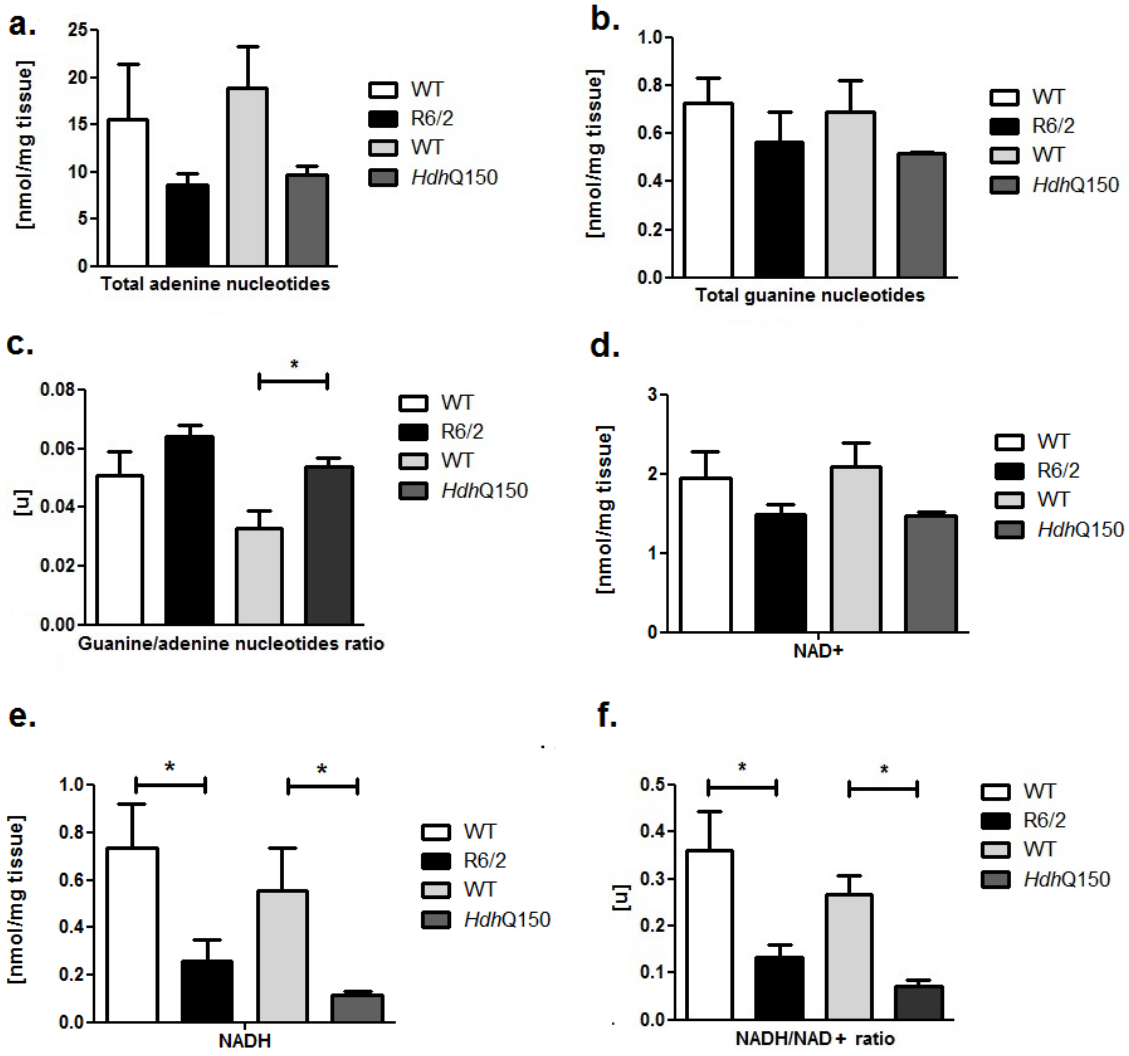


Figure 2

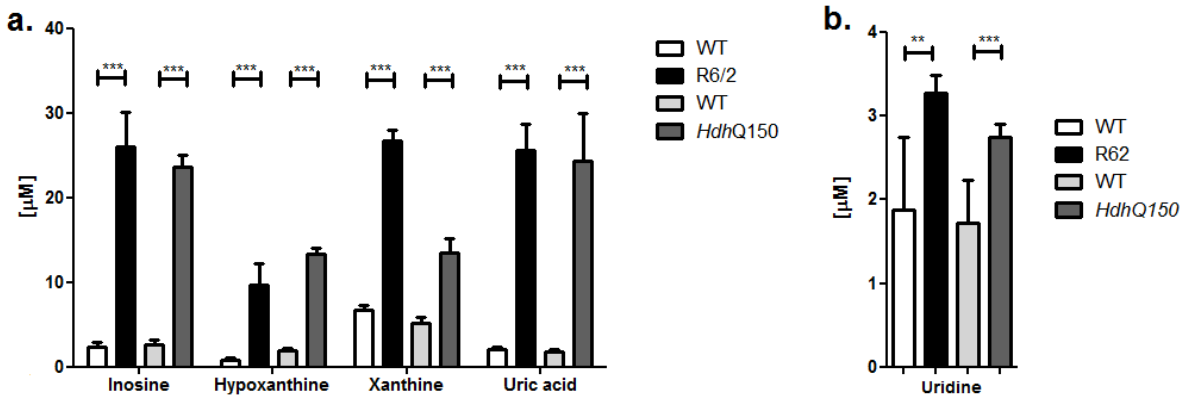

a.
[µM]
40
30
20
10
0
***
Inosine
Hypoxanthine
Xanthine
Uric acid
WT
R6/2
WT
HdhQ150
b.
[µM]
4
3
2
1
0
**
***
Uridine
WT
R62
WT
HdhQ150

Figure 3

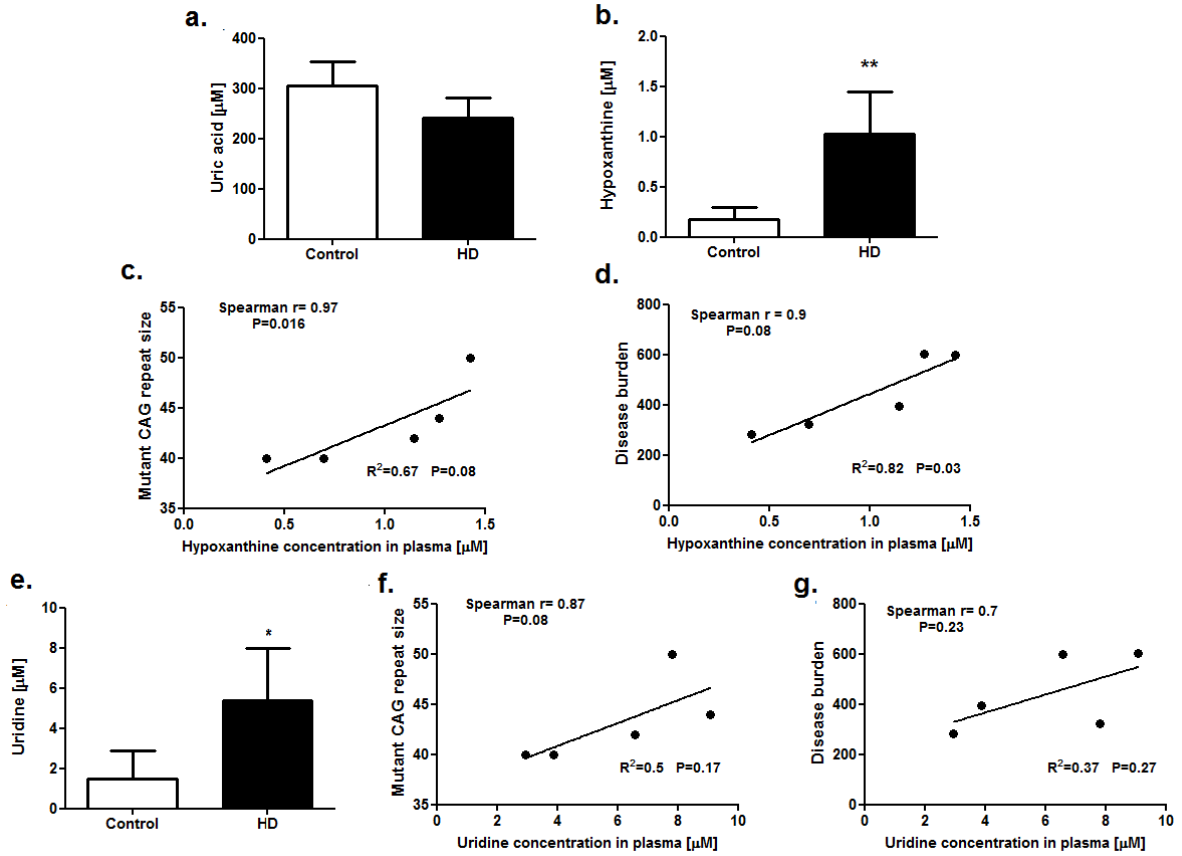

a.
Uric acid [µM]
400
300
200
100
0
Control
HD
b.
Hypoxanthine [µM]
2.0
1.5
1.0
0.5
0.0
**
Control
HD
c.
Mutant CAG repeat size
55
50
45
40
35
Spearman r= 0.97
P=0.016
R2=0.67 P=0.08
0.0
0.5
1.0
1.5
Hypoxanthine concentration in plasma [µM]
d.
Disease burden
800
600
400
200
0
Spearman r = 0.9
P=0.08
R2=0.82 P=0.03
0.0
0.5
1.0
1.5
Hypoxanthine concentration in plasma [µM]
e.
Uridine [µM]
10
8
6
4
2
0
*
Control
HD
f.
Mutant CAG repeat size
55
50
45
40
35
Spearman r= 0.87
P=0.08
R2=0.5 P=0.17
0
2
4
6
8
10
Uridine concentration in plasma [µM]
g.
Disease burden
800
600
400
200
0
Spearman r= 0.7
P=0.23
R2=0.37 P=0.27
0
2
4
6
8
10
Uridine concentration in plasma [µM]

Figure 4

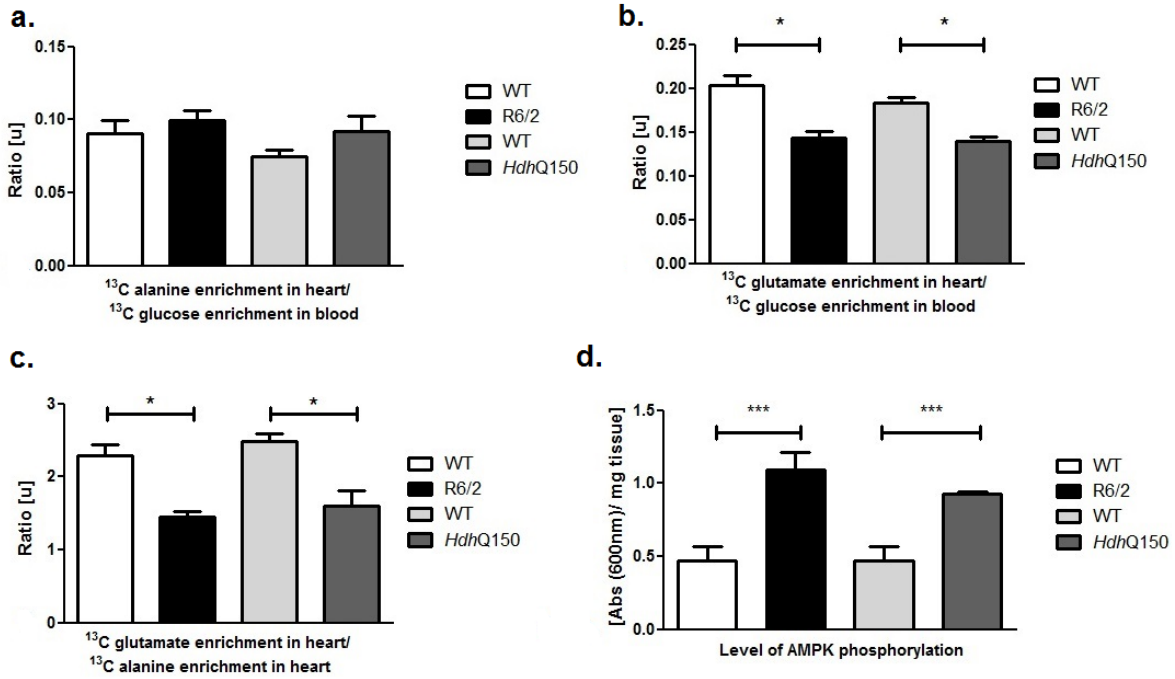

a.
0.15
0.10
0.05
0.00
Ratio [u]
WT
R6/2
WT
HdhQ150
13C alanine enrichment in heart/
13C glucose enrichment in blood
b.
*
*
0.25
0.20
0.15
0.10
0.05
0.00
Ratio [u]
WT
R6/2
WT
HdhQ150
13C glutamate enrichment in heart/
13C glucose enrichment in blood
c.
*
*
3
2
1
0
Ratio [u]
WT
R6/2
WT
HdhQ150
13C glutamate enrichment in heart/
13C alanine enrichment in heart
d.
***
***
1.5
1.0
0.5
0.0
[Abs (600nm)/ mg tissue]
WT
R6/2
WT
HdhQ150
Level of AMPK phosphorylation

Figure 5

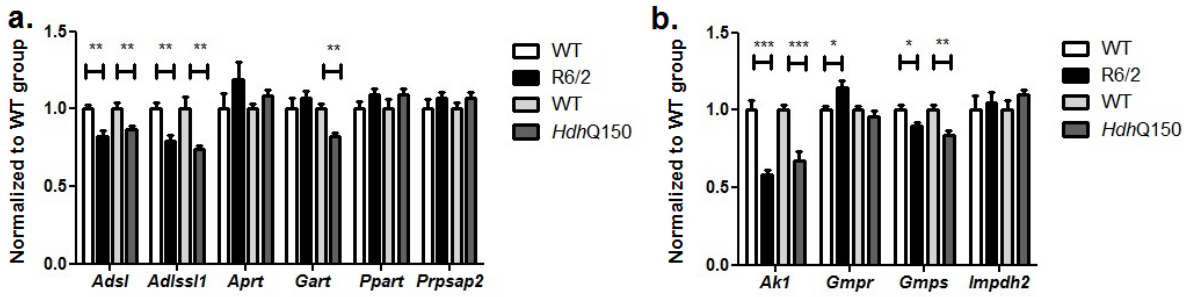

a.
Normalized to WT group
1.5
1.0
0.5
0.0
**
**
**
**
**
Adsl
Adlssl1
Aprt
Gart
Ppart
Prpsap2
WT
R6/2
WT
HdhQ150
b.
Normalized to WT group
1.5
1.0
0.5
0.0
***
***
*
*
**
Ak1
Gmpr
Gmps
Impdh2
WT
R6/2
WT
HdhQ150

Figure 6

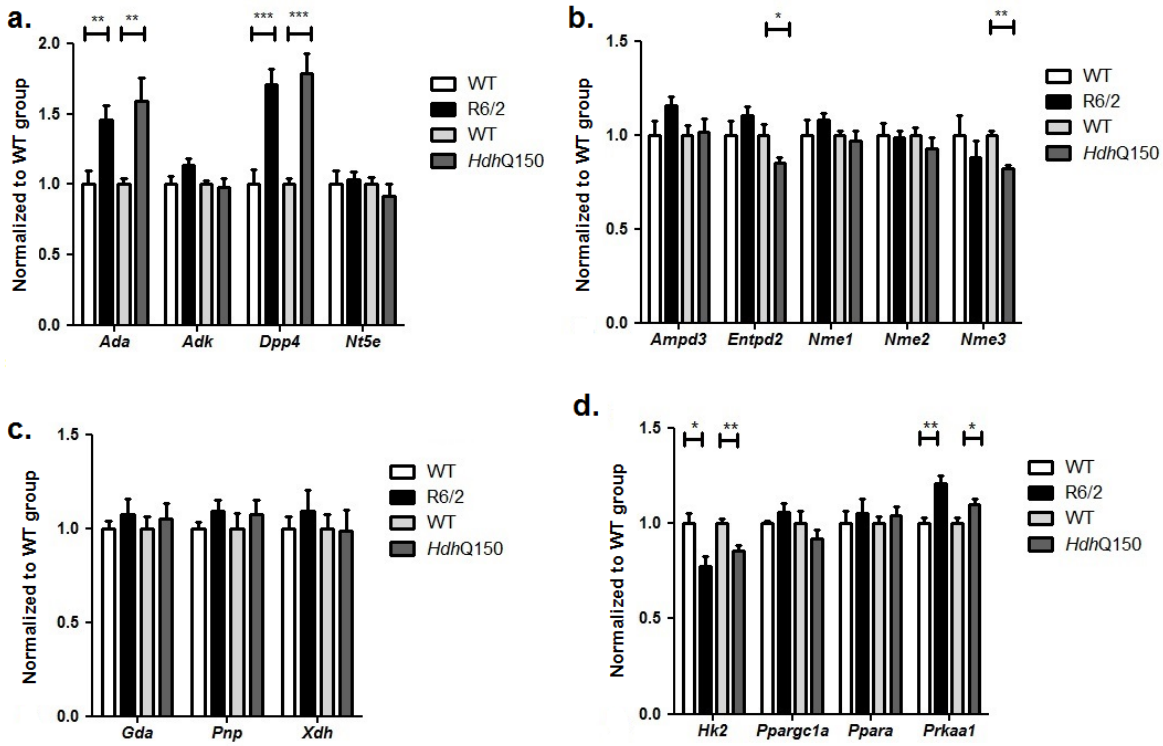

a.
b.
c.
d.
Normalized to WT group
WT
R6/2
WT
HdhQ150
Ada
Adk
Dpp4
Nt5e
Ampd3
Entpd2
Nme1
Nme2
Nme3
Gda
Pnp
Xdh
Hk2
Ppargc1a
Ppara
Prkaa1

Figure 7

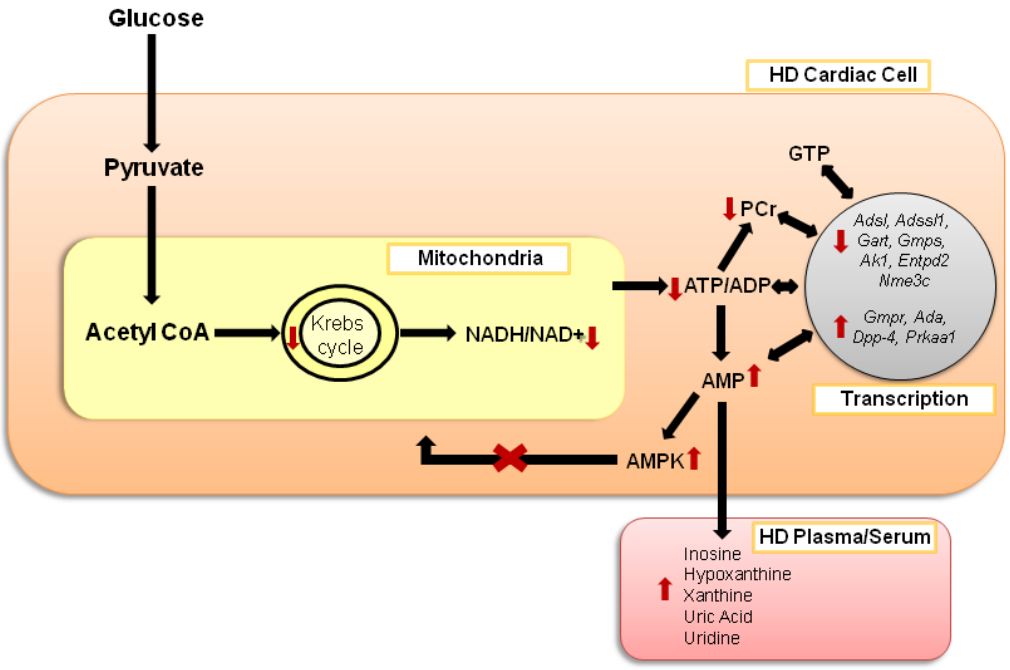

Glucose
HD Cardiac Cell
Pyruvate
GTP
PCr
Adsl, Adssl1, Gart, Gmps, Ak1, Entpd2 Nme3c
Mitochondria
ATP/ADP
Acetyl CoA
Krebs cycle
NADH/NAD+
Gmpr, Ada, Dpp-4, Prkaa1
AMP
Transcription
AMPK
HD Plasma/Serum
Inosine
Hypoxanthine
Xanthine
Uric Acid
Uridine

Figure 8

SUPPLEMENTARY TABLES AND FIGURES

An impaired metabolism of nucleotides underpins a novel mechanism of cardiac remodeling leading to Huntington's disease related cardiomyopathy. Marta Toczek, Daniel Zielonka, Paulina Zukowska, Jerzy T Marcinkowski, Ewa Slominska, Mark Isalan, Ryszard T. Smolenski, Michal Mielcarek

	ATP [μM]	ADP [μM]	NAD+ [μM]
WT	7.2 ± 5.1	2.8 ± 0.13	4.7 ± 1.4
R6/2	8.5 ± 4.9	4.5 ± 0.11	4.1 ± 1.4
WT	8.6 ± 3.6	6.1 ± 3.1	3.9 ± 1.5
***Hdh*Q150**	8.5 ± 3.3	6.6 ± 1.9	2.6 ± 1.5

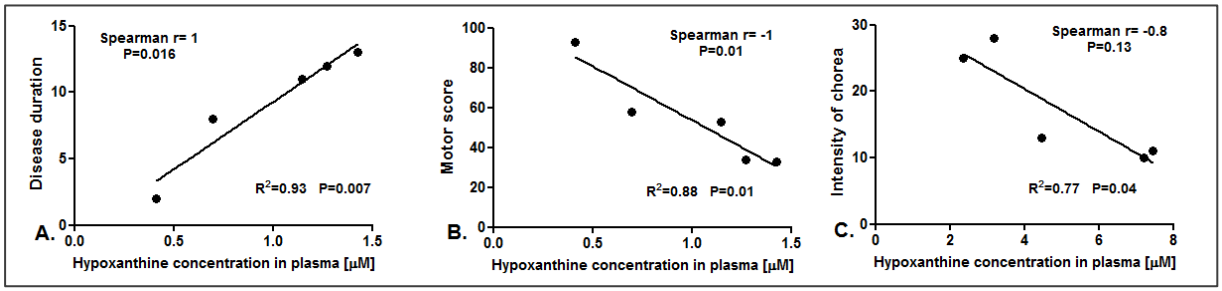
Supplementary Table 1. Adenine nucleotides (ATP, ADP) and NAD+ levels in sera from mice. Results presented as mean ± SD, n=5.

	HD patients	Control
Male/ female	4/1	3/2
Age [y]	59 ± 11	44 ± 8
Body mass [kg]	67 ± 10	68 ± 12
BMI	23 ± 2	23 ± 3
Mutant CAG repeat size	43 ± 4	-
Age of onset [y]	46 ± 10	-
Disease duration [y]	12 ± 4	-
Disease burden	440 ± 152	-
Motor score	54 ± 24	-
Intensity of chorea	17 ± 8	-

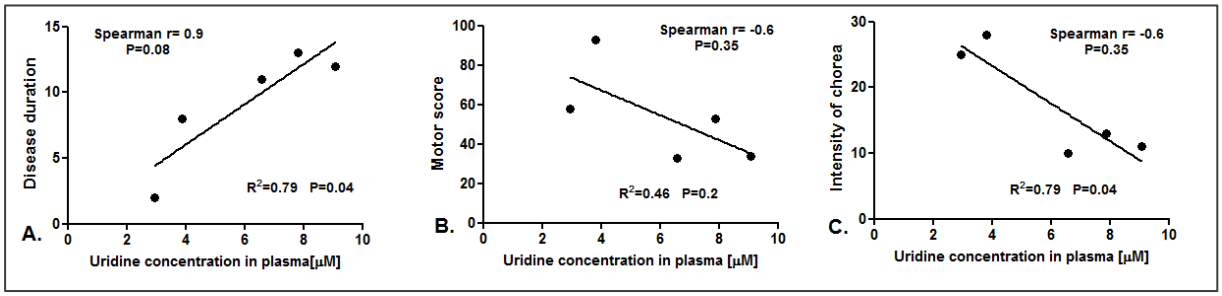
Supplementary Table 2. Characteristics of the study population.
One of the HD patients has been diagnosed with ischemic heart conditions. All other HD patients and healthy controls were cardiologically normal. Results presented as mean ± SD, n=5.

	ATP [µM]	ADP [µM]	NAD+ [µM]
HD patients	1.71 ± 1.15 *	1.27 ± 0.46	1.51 ± 0.46
Control	3.22 ± 0.71	1.24 ± 0.75	2.66 ± 1.21

Supplementary Table 3. Adenine nucleotides (ATP, ADP) and NAD+ levels in HD patients and control plasma. Results presented as mean ± SD, n=5, * $p<0.05$.



Supplementary Figure 1. Correlation between hypoxanthine concentration in HD patients' plasma and: A. Disease duration. **B.** Motor score. **C.** Intensity of chorea. n=5.



Supplementary Figure 2. Correlation of uridine concentration in HD patients' plasma and: A. Disease duration. **B.** Motor score. **C.** Intensity of chorea. n=5.

Metabolite concentration in serum/plasma	R6/2 HD mouse model vs. control mouse	*Hdh*Q150 HD mouse model vs. control mouse	HD patients vs. healthy control
ATP	No changes	No changes	↓
Hypoxanthine	↑	↑	↑
Uric acid	↑	↑	No changes
Uridine	↑	↑	↑

Supplementary Table 3. Summary of metabolites' concentrations in HD mouse models serum and HD patients' plasma.